Mol. Cryst. Liq. Cryst. 1995, Vol. 261, pp. 113–122
Reprints available directly from the publisher
Photocopying permitted by license only

OPTICALLY INDUCED REORIENTATION IN NEMATICS DOPED BY CHIRAL AGENTS

PASQUALINO MADDALENA, GIOVANNA ARNONE, GIANCARLO ABBATE, LORENZO MARRUCCI, and ENRICO SANTAMATO
Dipartimento di scienze Fisiche, Università di Napoli
Pad.20, Mostra d'Oltremare, 80125, Napoli, Italy

Abstract We have studied the optical Fréedericks transition for normal incidence in chiral-nematic mixtures in cells coated for homeotropic alignment. In the case of linear polarization of the incident beam two optical thresholds were observed: the first one is second-order and the second one is first-order, accompanied by very large hysteresis loop. In the case of circular polarization, the double-threshold feature was noticed only when the light elicity was the same as the sample chirality. When the elicity is opposite to the chirality, only one second order reorientational transition is produced. The experimental results were found only in partial agreement with the predictions of a simple plane-wave model.

INTRODUCTION

Small quantities of chiral molecules added to a nematic host can induce an helix structure in the material[1]. The Helix Twisting Power (HTP) of the chiral dopant is defined as

$$HTP = (p_0 c)^{-1}$$

where c is the dopant concentration and p_0 is the induced chiral helix pitch. For small concentration c, the HTP is independent of c and depends on the guest-host substances and temperature only[2]. Chiral doped nematics have been widely used in twisted or super twisted cells for displays. These devices are usually realized in the planar alignment, and only a few works have been performed on homeotropically aligned chiral nematic cells. Nevertheless, this case is interesting because

of the incompatibility between homeotropic alignment and helix formation. We expect, in fact, that for very thin samples the boundary forces are prevailing and the homeotropic alignment is stabilized. For thicker samples, or for larger chiral concentration c, the helix structure is formed, leading to the formation of twisted domains. The domains can be eventually quenched by applying a suitable electric field[3,4]. In a recent experiment, however, it was proved that the *optical* reorientation of nematic-cholesteric mixtures does not lead to domain formation, thus maintaining the good optical transparency of the sample[5]. The lacking of bubble formation is due probably to the small cross section ($\simeq 100\mu$m) of the reoriented area. The optical reorientation process in the presence of chiral dopant is quite different from usual Optical Fréedericksz Transition (OFT) in pure nematic: two thresholds have been observed, one second-order, as in pure nematics, and one, much larger, first-order[5]. This last transition is accompanied by a very large hysteresis loop, where all-optical intrinsic Optical Bistability (OB) is obtained.

In this work we present a further study of the optical reorientation in cholesteric-nematic mixtures, confirming the occurrence of the double-threshold feature not only in the case of linear polarization of the laser beam, but also in the case of circular polarization having the same elicity of the chiral helix. For laser polarization having opposite elicity, instead, only one second-order OFT was observed. This provides a very simple method to determine the chirality sign of the dopant molecules, especially in the case of very low concentration where the pitch p_0 is too large to be measured directly by Cano's wedge or other polarimetric methods.

EXPERIMENT

In our experiments we used mixtures of nematic *E7* and cholesteric *C15* and *CB15* liquid crystals from *MERK-BDH*. These cholesteric dopants have opposite chirality. The samples were prepared by mixing the components above the clearing temperature of *E7* ($\simeq 60$°C). The hot mixture was then introduced by capillarity into cells made of two parallel glass plates coated with *CTAB* for homeotropic alignment and separated by mylar strips. The cells were finally cooled slowly

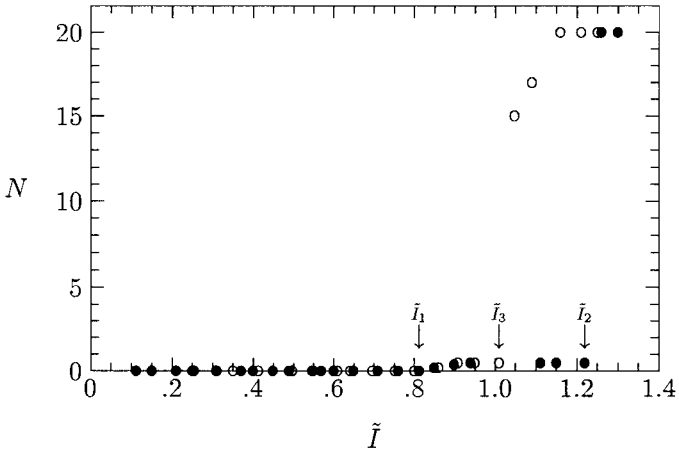

FIGURE 1 Number of rings N as function of reduced intensity $\tilde{I}$ for *E7-CB15* mixture with chirality $\tilde{q} = 0.45$. • increasing intensity. ○ decreasing intensity. The temperature and film thickness were $T = 25°C$ and $L = 50\mu m$, respectively.

towards the nematic phase. The cholesteric concentration was taken below the critical value for the given thickness and temperature, so that the initial alignment was homeotropic on the whole sample area. We made samples having thicknesses of $50\mu m$ and $110\mu m$. The critical concentration of *C15* at 25°C was found $1.75 \pm 0.01\%$ for $50\mu m$ thick samples and $0.82 \pm 0.01\%$ for $110\mu m$ thick samples. For *CB15* the critical concentration in $50\mu m$ samples was found to be $0.21 \pm 0.01\%$. We were not able to measure the critical concentration of *CB15* in $110\mu m$ samples, because of the very low concentration required. These data correspond to a $HTP = 82 cm^{-1}$ for *C15* and to a $HTP = 700 cm^{-1}$ for *CB15*. When the samples were prepared with chiral concentration below the critical value, the homeotropic alignment was found to be stable in the whole nematic range of *E7* up to its clearing temperature (60°)C, contrarily to what previously reported[5]. We think that the formation of the fingerprint texture observed in Ref.[5] was due to contamination by the epoxy glue used to seal the cells. During the experiments the sample temperature was held fixed at $(25 \pm 0.1)°C$ by putting it into an electronically stabilized oven.

The *OFT* was investigated at normal incidence by using a $3W$ argon laser

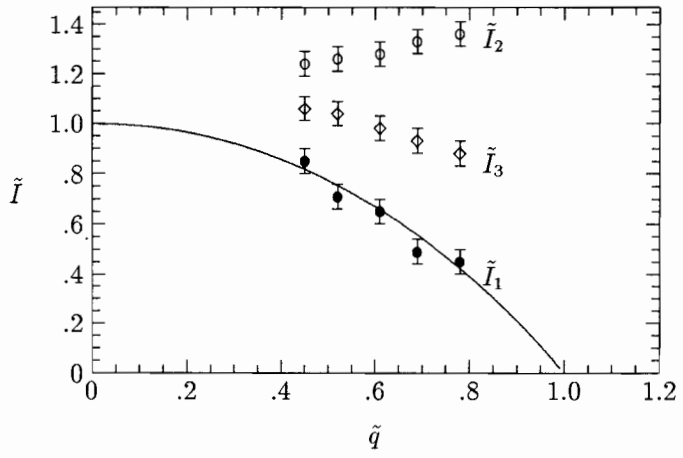

FIGURE 2 The three thresholds as functions of chirality $\tilde{q}$ for *E7-CB15* mixture and linear polarization. The full line is from the linearized theory. The temperature and film thickness were $T = 25°C$ and $L = 50\mu m$, respectively.

working at $\lambda = 514.5nm$ in TEM_{00} mode. The laser beam was focused onto the sample to a measured $1/e^2$ intensity radius of $(82 \pm 2)\mu m$. Linear and circular polarizations were obtained by means of appropriate polarizers and birefringent plates. The laser-induced reorientation in the sample was monitored either observing the number of diffraction rings in the far field beyond the sample or determining the polarization state of the light passing through a $1mm^2$ aperture located at the center of the far field pattern. Both the polarization ellipse orientation angle ψ and the ellipticity e were measured by an ellipsometric null method[6].

Using different samples we always found consistent results. All data reported in this work refer, however, to $50\mu m$ thick samples made of a mixture of nematic *E7* and cholesteric *CB15*. The behavior of the sample birefringence for linear polarization is shown in Fig. 1, where the number of diffraction rings in the far field pattern is plotted as a function of the laser intensity. The three intensity thresholds $\tilde{I}_1$, $\tilde{I}_2$ and $\tilde{I}_3$ are pointed out by arrows. In the figure, the intensity is normalized with respect to the threshold I_0 of the *OFT* measured in a pure *E7* nematic sample having the same thickness. At the first critical threshold $\tilde{I}_1$,

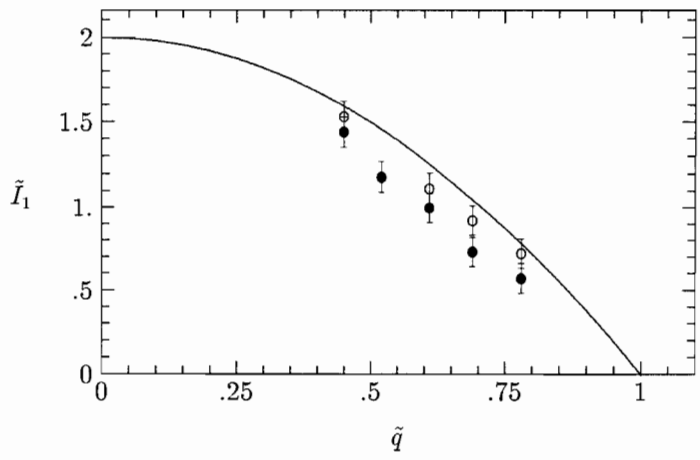

FIGURE 3 First threshold reduced intensity as a function of chirality $\tilde{q}$ for *E7-CB15* mixture and circular polarization. • right-handed. ○ left-handed. The full line is from the linearized theory. The temperature and film thickness were $T = 25°C$ and $L = 50\mu m$, respectively.

the sample undergoes a second order *OFT* to a low splay-bend distortion state, where the sample birefringence is very small. The small birefringence state remains frozen over a large intensity range, as shown by the low-level *plateau* in Fig. 1, corresponding to about 0.5 ring in the far field. Only when the laser intensity reaches the second threshold $\tilde{I}_2$, the sample jumps up to a high birefringence state through a first order transition. The high distortion state remains stable even if the intensity is lowered, until, at the critical value $\tilde{I}_3$, the system relaxes back, by a first-order transition, to the small birefringence state. To put the system back in the initial undistorted state, the intensity must be further reduced below $\tilde{I}_1$.

The first threshold intensity $\tilde{I}_1$ is always lower than the *OFT* threshold I_0 in the pure sample, because of the presence of the chiral dopant tending to destabilize the initial homeotropic alignment. We expect, therefore, that the first instability threshold $\tilde{I}_1$ should be a decreasing function of the sample chirality. This is shown in Fig. 2, where $\tilde{I}_1$, $\tilde{I}_2$ and $\tilde{I}_3$ are reported as functions of the sample chirality parameter $\tilde{q}$, defined in the next section. We see that while $\tilde{I}_1$ decreases with chirality, both $\tilde{I}_2$, $\tilde{I}_3$ and their difference $\Delta\tilde{I} = \tilde{I}_2 - \tilde{I}_3$ are increasing functions

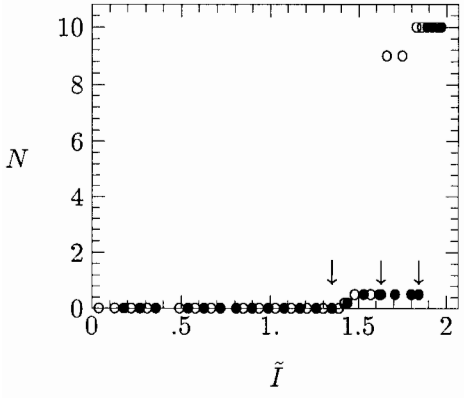

FIGURE 4 Number of rings N as a function of reduced intensity $\tilde{I}$ for circular polarization rotating as the chiral helix. • increasing intensity. o decreasing intensity. Other parameters are as in previous figures.

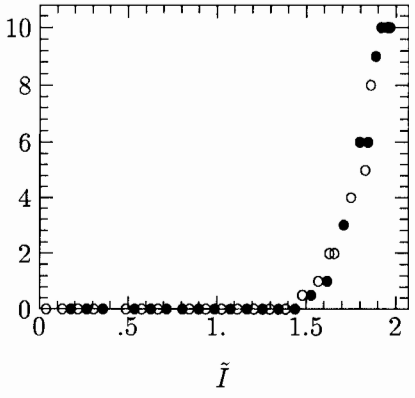

FIGURE 5 Number of rings N as a function of reduced intensity $\tilde{I}$ for circular polarization rotating opposite to the chiral helix. • increasing intensity. o decreasing intensity. Other parameters are as in previous figures.

of $\tilde{q}$. The quantity $\Delta\tilde{I}$ can be taken as a measure of the hysteresis region, where all-optical intrinsic OB is achieved. We notice that in chiral doped nematics the intrinsic OB range is more then one order of magnitude larger than the OB range obtained in pure nematic by applying a bias magnetic field[7].

The results for circular polarization are shown in Figs. 3, 4 and 5. Figure 3 reports the first threshold intensity for right-handed and left-handed circular polarization. Within the experimental errors the threshold intensity for the two polarizations is almost the same, although somewhat lower than the value provided by the linearized model (full line curve). This little discrepancy can be ascribed to thermal heating of the sample, altering the material constants. We see that even in the circular polarization case the threshold decreases with chirality starting from a value close to twice the threshold for linear polarization.

The above threshold behavior is however quite different for the two circular polarizations, as it can be seen in Figs. 4 and 5, where vertical arrows indicate the observed thresholds. Both figures refer to the same chirality parameter $\tilde{q} = 0.45$,

corresponding to a helix pitch of 150μm. When the light polarization rotates in the same direction as the chiral helix of the sample, the three-threshold feature with first-order transition and large hysteresis loop is clearly visible as shown in Fig.4. In the case of opposite circular polarization, instead, a single second-order *OFT* is observed, as in pure nematic. We observed consistent behavior either changing the elicity of the light polarization or changing the chirality of the dopant, passing from *CB15* to *C15*. The effect is amazing, considering the very large pitch of the helix, that can be up to three or four times the sample thickness.

THE MODEL

To describe the *OFT* in chiral-doped nematic we used a straightforward generalization of our previous model describing the optical reorientation in pure host for normal incidence and generic elliptical polarization of the input beam[8]. The generalization consists simply of adding to the elastic part of the free energy a chiral term

$$-\left(\frac{2\pi k_{22}}{p_0}\right)\sin^2\theta\,\frac{d\phi}{dz},$$

where p_0 is the helix pitch as obtained from the dopant *HPT* and concentration. Corresponding chiral terms will appear therefore in the expressions for the elastic torque per unit volume. The final set of equations is similar to the one reported in Ref.[8], to which we refer also for the symbol notation. The steady state torque equations can be linearized around the undistorted homeotropic alignment, obtaining the following expressions for the first threshold intensity I_1 for the *OFT*:

$$\begin{aligned} \tilde{I}_1 &= 4\tilde{q}^2\left(\tfrac{2}{\pi\Delta}\right)\tan\left(\tfrac{\pi\Delta}{2}\right) \quad \text{(linear polarization)} \\ \tilde{I}_1 &= 2(1-\tilde{q}^2) \qquad\qquad\quad \text{(circular polarization)} \end{aligned} \tag{1}$$

where

$$\Delta = \sqrt{\tilde{I}_1 + 4\tilde{q}^2}, \tag{2}$$

$$\tilde{q} = \frac{2k_{22}L}{k_{33}p_0} \tag{3}$$

and L is the sample thickness. The threshold intensity I_1 as obtained from Eqs.(1) is reported in full line in Figs. 2 and 3. The agreement with the experimental data

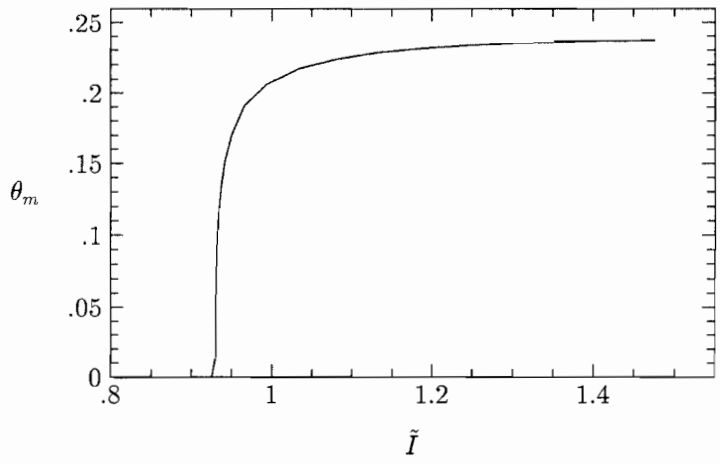

FIGURE 6 Maximum angle θ_m at the sample center as function of reduced intensity $\tilde{I}$.

is excellent.

We tried also to extend the model beyond the small distortion region by numerically integrating the torque equations both for steady and for time dependent states. In Fig.6 is reported the steady state value of the director tilt angle θ_m at the sample center as a function of the reduced intensity $\tilde{I}$. The following material constants have been used in the calculation: $k_{11} = 11 \times 10^{-7}$ dyne, $k_{22} = 5.8 \times 10^{-7}$ dyne, $k_{33} = 16 \times 10^{-7}$ dyne, $L = 50\mu$m, $\tilde{q} = 0.45$, $n_e = 1.74$, $n_o = 1.52$. The angle θ_m is a good measure of the laser-induced molecular distortion. The saturation value of θ_m is here $\theta_m = 0.237$, much lower than the saturation value of $\pi/2$ occurring in pure samples. The birefringence freezing effect is then confirmed by the model. Nevertheless, some discrepancies also occur. For example, the model does not reproduce the second transition at I_2 to the high distorted state neither the bistability loop. Moreover, in the case of a linearly polarized laser beam, the output polarization, although linear, should be rotated with respect to the laser, because of the twisting of the molecular director inside the sample (see Fig.7). We made several attempts to observe the polarization rotation, but we always found the light polarization at the center of the far field pattern being the same as the

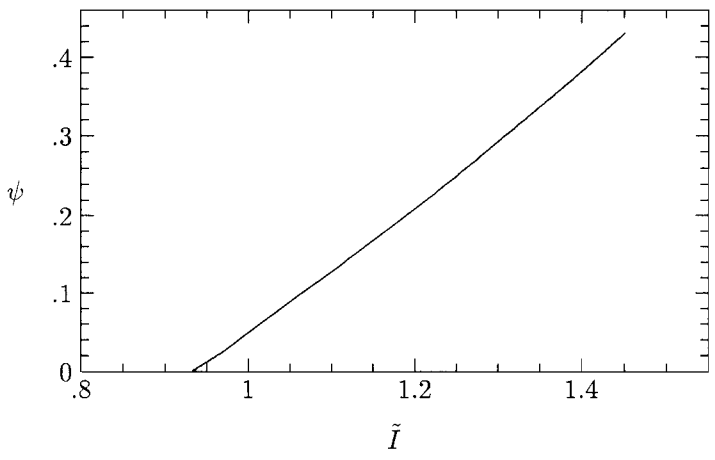

FIGURE 7 Theoretical value of the polarization ellipse angle ψ at the sample exit as a function of the reduced intensity $\tilde{I}$

input light. Also in the case of circular polarization, our model was found only in partial agreement with the experiments. The accordance was very good for the first threshold value and for the case of circular polarization opposite to the helix winding, where the single second-order *OFT* was observed. In the case of circular polarization having the same elicity of the helix, instead, our model predicts time oscillating states that were never seen in the experiments.

CONCLUSIONS

We have presented an experimental study of the *OFT* in chiral-doped nematic at normal incidence. The occurrence of new qualitative features, as the large optical bistability loops and first-order transitions, was confirmed both for linear and circular polarization, having the same elicity of the sample chirality. In the case of opposite elicity, a single second-order transition, similar to the one observed in pure samples, was instead observed. A model obtained by a straightforward generalization of a previous one, working very well in the case of pure nematic, was used to describe the phenomena. The agreement was good as long as it concerns the first threshold values and the birefringence freezing effect. Our model

was nevertheless unable to reproduce the observed hysteresis loops and first-order transitions. Moreover, we failed to observe the expected rotation of the light polarization plane and the occurrence of oscillating states for circular polarization. These discrepancies could be due to the fact that the chiral helix develops in a direction different from the normal to the film (z-axis). Further experimental investigations to check out the helix axis direction in the sample and corresponding improvements of our model to include the transverse coordinates are now in progress.

ACKNOWLEDGMENTS

This work was supported by Ministero dell'Università e della Ricerca Scientifica and by Consiglio Nazionale delle Ricerche under a special coordinate project.

REFERENCES

1. S. Chandrasekhar, Liquid crystals, Cambridge University Press, Cambridge, 1977, Chap. 4.
2. V. G. Bhide, S. Chandra, S. C. Jain, R. J. Mendekar, J. Appl. Phys., 47, 120 (1976).
3. W. E. L. Hass, and J. E. Adams, Appl. Phys. Lett., 25, 535 (1974)
4. V. G. Bhide, S. C. Jain, S. Chandra, J. Appl. Phys., 48, 3349 (1977).
5. G. Abbate, A. Ferraiuolo, P. Maddalena, L. Marrucci, and E. Santamato, Liquid Cryst., 14, 1431 (1993).
6. R. M. A. Azzam and N. M. Bashara, Ellipsometry and polarized light, North-Holland, New York, 1977.
7. A. J. Karn, S. M. Arakelian, Y. R. Shen, H. L. Ong, Phys. Rev. Lett., 57, 448 (1986).
8. E. Santamato, G. Abbate, P. Maddalena, Phys. Rev. A, 38, 4323 (1988).